

# Anatomy of a Flaring Proto-Planetary Disk Around a Young Intermediate-Mass Star

Pierre-Olivier Lagage,<sup>1\*</sup> Coralie Doucet,<sup>1</sup> Eric Pantin,<sup>1</sup> Emilie Habart,<sup>2</sup> Gaspard Duchêne,<sup>3</sup> François Ménard,<sup>3</sup> Christophe Pinte,<sup>3</sup> Sébastien Charnoz,<sup>1</sup> Jan-Willem Pel<sup>4,5</sup>

Although planets are being discovered around stars more massive than the Sun, information about the proto-planetary disks where such planets have built up is sparse. We have imaged mid-infrared emission from polycyclic aromatic hydrocarbons at the surface of the disk surrounding the young intermediate-mass star HD 97048 and characterized the disk. The disk is in an early stage of evolution, as indicated by its large content of dust and its hydrostatic flared geometry, indicative of the presence of a large amount of gas that is well mixed with dust and gravitationally stable. The disk is a precursor of debris disks found around more-evolved A stars such as  $\beta$ -Pictoris and provides the rare opportunity to witness the conditions prevailing before (or during) planet formation.

Based on the growing number of known planetary systems (1) and on the wealth of observations of disks around young stellar objects (2, 3), it is now well established that planets around main-sequence solar-type stars form in massive, gaseous, and dusty proto-planetary disks that survive for several million years around the nascent stars (4). The situation is less clear for stars of more than  $\approx 2$  solar masses. Such stars have a much higher luminosity than solar-type stars, and, according to models, processes such as photoevaporation may be at work clearing the inner disk in a few million years (5). Whereas radial velocity surveys have just started to reveal planets around stars about twice as massive as the Sun (6), current imaging observations of proto-planetary disks around stars with such a mass remain very sparse (3). Most resolved disks are debris disks around A-type stars that are on the main sequence (3, 7). In such disks, the gas has been dispersed, and planets have probably formed already, as indicated by asymmetries and ring-like structures in the disks (4). The lack of well-resolved images of proto-planetary disks around much younger A stars, still on the pre-main sequence, is due to the fact that such stars are

less numerous than their solar-type equivalents, the T-Tauri stars, and in general are located farther away from Earth. As a result, the fallback option to estimate the properties of the disks around these stars has been to fit their spectral energy distribution (SED). By doing so, the pre-main sequence stars of intermediate mass ( $\approx 2$  to 4 solar masses), the so-called Herbig Ae (HAe) stars, have been classified in two groups: Group I members feature a rising SED in the 10- to 60-micrometer ( $\mu\text{m}$ ) wavelength range [mid- and far-infrared (IR)], whereas group II members feature a flatter SED (8). The preferred physical

interpretation is that group I disks are flared and group II disks are geometrically flatter. A flaring disk is a disk in which the ratio of disk thickness to the distance to the star,  $H/r$ , increases with  $r$ ; then, any point at the surface of such disks receives direct light from the star, and the disk intercepts a substantial part of the stellar radiation out to large distances. Half of the intercepted light is reradiated away from the disk, and the other half is reradiated down into the disk's deeper layers, providing additional heating to the dust in the optically thick disk interior, which reradiates in the mid-IR, far-IR, and submillimeter wavelengths. The information provided by SED fitting remains limited, because numerous disk parameters are assumed or have not been conclusively determined (9). Direct measurements from imaging are therefore required to unambiguously constrain more parameters, such as the overall shape (outer radius and height) of the disk, which determines the amount of starlight captured by the disk. Imaging of disks has been obtained either by observations of the starlight dust scattering (in the visible and near-IR radiation) or of dust thermal emission or by CO lines in the millimeter observations (3, 10, 11). Scattered starlight observations suffer from the limited contrast offered by imaging devices, and millimeter observations suffer from limited spatial resolution.

A new approach to image disks around HAe stars exploits the fact that about half of them have prominent IR emission bands (IEBs) at 3.3, 6.2, 7.7, 8.6, and 11.3  $\mu\text{m}$  (12). These IEBs are believed to arise from the cooling of transiently heated polycyclic aromatic hydrocarbons (PAHs),

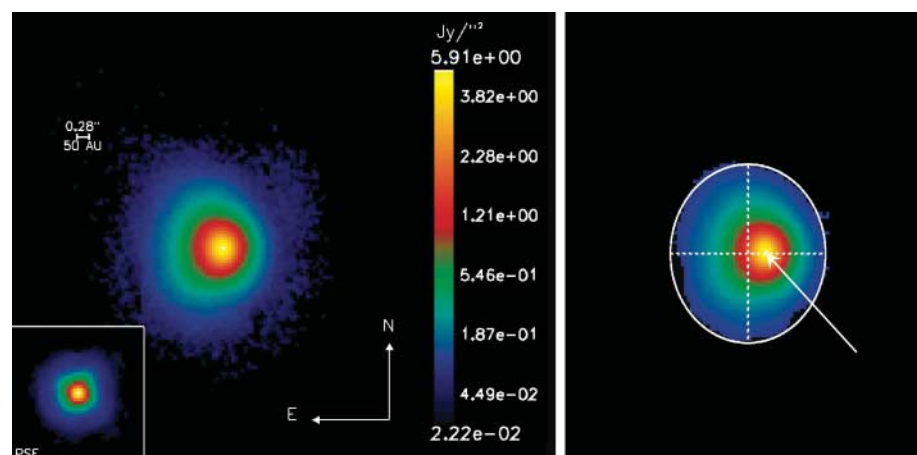


**Fig. 1. (Left)** VISIR false-color image of the emission from the circumstellar material surrounding the HAe star HD 97048 after a deep exposure (36 min). VISIR's PAH1 filter was used; it is centered on the IEB at 8.6  $\mu\text{m}$  and has a full width at half maximum (FWHM) of 0.42  $\mu\text{m}$ . The emission is widely extended, as compared with the point spread function (PSF) (inset) obtained from the observation of the pointlike reference star HD 102964, which was made 15 min before the observation of HD 97048. The measured FWHM of 0.33'' is close to the diffraction limit of 0.28'', also indicated on the figure. The pixel size is 75 milli-arc sec. The noise level is 1.6 millijansky (mJy)/arc sec<sup>2</sup>. The photometry, calibrated with HD 102964, yields a total flux of 5.75 ( $\pm 0.2$ ) Jy. **(Right)** Same image but with a cut at the brightness level of  $4.4 \times 10^{-3}$  Jy/arc sec<sup>2</sup> and a fit of the edge of the image by an ellipse. The dashed lines show the ellipse axis; the ellipse center is offset eastward from the peak flux, as indicated by the arrow.

<sup>1</sup>Laboratoire de l'Astrophysique des Interactions multi-échelles, Unité Mixte de Recherche N° 7158 [Commissariat à l'Energie Atomique (CEA), CNRS, Université Paris 7], Direction des Sciences de la Matière (DSM)/Laboratoire de recherches sur les lois fondamentales de l'Univers (DAPNIA)/Service d'Astrophysique, CEA Saclay, F-91191 Gif-sur-Yvette Cedex, France. <sup>2</sup>Institut d'Astrophysique Spatiale, F-91405, Orsay Cedex, France. <sup>3</sup>Laboratoire d'Astrophysique de Grenoble, CNRS/Université Joseph Fourier, Unité Mixte de Recherche N° 5571, Boîte Postale 53, F-38041 Grenoble Cedex 9, France. <sup>4</sup>Netherlands Foundation for Research in Astronomy, Dwingeloo, Netherlands. <sup>5</sup>University of Groningen, Groningen, Netherlands.

\*To whom correspondence should be addressed. E-mail: Pierre-Olivier.Lagage@cea.fr

which can be excited by the intense stellar ultraviolet radiation (13). For a flaring disk, the PAHs at the surface of the disk are in direct view of the central star and can be excited; the resulting IEB emission provides distinguishing information on the disk structure up to large distances from the star. In addition, observing in the mid-IR wavelength alleviates the problem of too much contrast between the photospheric and disk emission. We have thus undertaken a program of imaging “nearby” H Ae stars with VISIR (very large telescope imager and spectrometer in the mid-IR) at the European Southern Observatory (ESO) (14). One of the first targets was HD 97048, a nearby group I H Ae star of spectral type Be9.5/A0 located in the Chameleon I dark cloud, at a distance of 180 parsecs (15). The star has a temperature of 10,000 K, a luminosity ( $L_{\odot}$ ) of 40 solar luminosities, and a mass ( $M_{\odot}$ ) of 2.5 solar masses (15). It is surrounded by a large amount of circumstellar material left from the star formation process, as indicated by the large IR excess ( $L_{\text{IR}}$ ) observed in the SED [ $L_{\text{IR}} \sim 0.40 L_{\odot}$ ] (16). Mid-IR-extended emission has been detected on scales of a few thousand astronomical units and modeled as originating from a dust shell with an inner cavity radius of 180 AU (17). Recent long-slit mid-IR spectroscopic observations have revealed a strong resolved emission from the inner region (18). Imaging this region with the high-angular resolution offered by a 8-m-size telescope would be a direct way to assess whether HD 97048 is surrounded by a flaring disk, as expected from its rising mid-IR and far-IR SED (12).

The observations of HD 97048, conducted on 17 and 19 June 2005, were performed with filters centered on the IEB at 8.6  $\mu\text{m}$  and on the adjacent continuum at 9  $\mu\text{m}$ . The classical mid-IR observing technique of “chopping and nodding” was used, with a chopper throw of 10'' (north-south) and a nodding throw of 8'' (east-west). The 8.6- $\mu\text{m}$  image (Fig. 1) reveals a large extended emission with a strong east-west asymmetry; the brightness isophotal contours

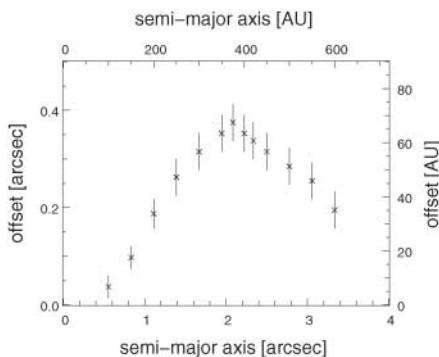


**Fig. 2.** Offset from the peak flux of the center of the ellipses fitting the image of HD 97048 at various brightness level cuts, as a function of the length of the ellipse semi-major axis (fig. S1). Error bars indicate the uncertainties from ellipse fitting.

are elliptical in shape, and the ellipse centers are offset from the peak of emission. The offset increases when lowering isophotal contours up to a semi-major axis of 2.1'', (Fig. 2 and fig. S1). Such features are characteristic of a flaring disk, vertically optically thick at the wavelength of the observations and inclined to the line of sight (Fig. 3). Beyond 2.1'', the offsets decrease. One possible explanation is that the disk then becomes vertically less optically thick. However, as an alternative explanation, the increasing contribution from the shell emission cannot be disregarded (17). We therefore restricted our study to the regions  $< 2.1''$ , corresponding to an astrocetric distance of 370 AU.

To retrieve quantitative information about the disk flaring in these regions, we have fitted the east and west brightness profiles with a simplified model. In this model, the PAH-emitting region is only located at the surface of the disk, whose surface scale height  $H_s$  varies with the astrocetric distance following a power law  $H_s(r) = H_0 (r/r_0)^\beta$ , where  $H_0$  is the disk surface height at the astrocetric distance  $r_0$  and  $\beta$  is the

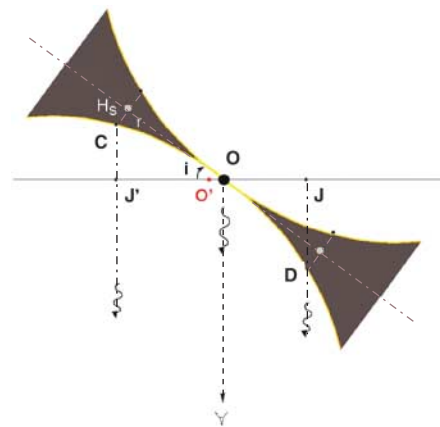


**Fig. 3.** Sketch of a slice of a flaring disk. The observer is viewing the disk from below (eye symbol). The disk is inclined, from pole-on, by an angle  $i$ . The disk is optically thick to the ultraviolet and visible starlight along its midplane so that the PAH emission only arises from the disk “surfaces,” indicated in yellow. When the disk is also optically thick vertically at the wavelengths of the observations (here in the mid-IR), only the front disk surface is seen by the observer. Consider two points C and D of the front disk surface, located at equal distances from the star (black circle at O). Because of projection effects, the observer views the center of emission from C and D at O' (red circle), between J and J', which is offset from O. For a flaring disk, the disk height  $H_s$  increases with the distance  $r$  to the star, so that the apparent offset increases, as observed for HD 97048. When the disk is vertically optically thin, the front and bottom disk surfaces are both observable, and the disk appears symmetrical with respect to the star. Curved arrows indicate that electromagnetic radiation is emitted toward the observer; gray circles indicate the projection of point C or D onto the disk midplane.

flaring index. We further assumed that the spatial variation of the flux intensity  $I$  follows a power law  $I(r) = I_0 (r/r_0)^\delta$ , where  $I_0$  is the intensity at  $r_0$  and  $\delta$  is the power law index. This hypothesis is only valid once the continuum emission contribution in the filter at 8.6  $\mu\text{m}$  has been removed, which we have done by extrapolating the continuum emission observed at 9  $\mu\text{m}$  (fig. S2). The result of the fit is shown in Fig. 4;  $\delta$  for the intensity is found to be  $-2.3 (+0.2/-0.06)$ , close to the expectation of an index value of  $-2$  for PAH emission (fig. S2), and the disk inclination is  $42.8 (+0.8/-2.5)$  degrees from pole-on. The scale height  $H_0$  is 51.3  $(+0.7/-3.3)$  AU at  $r_0 = 135$  AU and  $\beta$  is  $1.26 (\pm 0.05)$ , in agreement with the value expected from hydrostatic, radiative equilibrium models of passive flared disks (9). In these models, the flaring structure is supported by the gas, whose vertical scale height  $H_g$  is governed by the balance between gas pressure and gravitational pull; the dust plays the key role to capture the starlight and then heat the gas collisionally.  $H_s$  corresponds to the upper layers of the disk, where the starlight is intercepted by dust, and is about four times as large as the gas height (9). Given the disk's outer radius and scale height, the calculated amount of starlight captured by the disk is 43%, in good agreement with the observed IR excess (16).

Our observations also provide information about the disk mass. From the observed west-east asymmetry, we can infer that the vertical optical thickness  $\tau$  at 370 AU is at least 1, implying that, at 370 AU, the dust mass surface density  $\Sigma_0$  is at least  $1/1600 \text{ g cm}^{-2}$  (19). Assuming that the astrocetric variation of mass

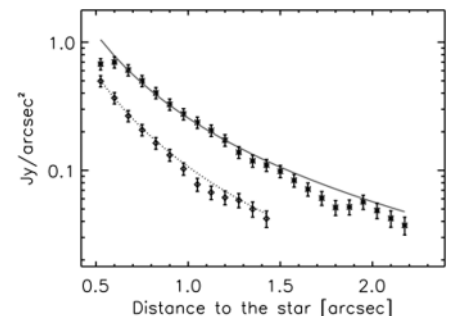


**Fig. 4.** Fit of the observed east (upper data and solid curve) and west (lower data and dotted line) intensity profiles with a simple flaring disk model. The reduced  $\chi^2$  value of the fit is 0.3, well below 1. The error bars indicate the uncertainties in the data due to the background noise and photometric uncertainties from the continuum subtraction ( $\pm 5\%$  for each image). The range in model parameters has been calculated by exploring the parameter space, which leads to a reduced  $\chi^2 < 1$ . Below 0.5'', there is no data point, because it is impossible to disentangle reliably the IEB emission from the much larger continuum thermal emission. The angular distance to the star refers to the projected distance on the plane of the sky.

surface density  $\Sigma$  follows a power law  $\Sigma(r) = \Sigma_0 (r_{\text{AU}}/370)^q$ , with an index  $q$  equal to  $-3/2$ , as the one inferred for the solar nebula or for extrasolar nebulae (20, 21), we derived a disk dust mass of 40 Earth masses within 370 AU. This lower limit is compatible with the mass of 500 Earth masses derived from the observed 1.3-mm flux (22). The dust mass derived here is three to four orders of magnitude larger than the dust mass observed in debris disks and Kuiper belt-like structures found around more-evolved A stars such as  $\beta$ -Pictoris, Vega, Fomalhaut, and HR 4796 (4). The dust around these Vega-like stars is thought to be produced by collisions of larger bodies, whose total mass in the case of  $\beta$ -Pictoris has been estimated to be on the order of 100 Earth masses (23). Therefore, the dust mass observed around HD 97048 is similar to the mass invoked for the (undetected) parent bodies in more-evolved systems. HD 97048's disk is thus most likely a precursor of debris disks observed around more-evolved A stars. This finding is coherent with the HD 97048 age of  $\sim 3$  million years, estimated from evolutionary tracks. Another argument in favor of the early evolutionary stage of the system is the presence of a large amount of gas required to support the flaring structure revealed by our observations. Part of the gas has been recently detected, thanks to observations of the molecular hydrogen emission at 2.12  $\mu\text{m}$  (24). Assuming that the canonical interstellar gas-to-dust mass ratio of 100 holds, we estimate a total minimum disk mass of 0.01 solar masses, like the estimated minimum mass for the proto-planetary disk around the Sun (20).

Because the disk surrounding HD 97048 has a mass surface density comparable to that of the minimum proto-planetary nebula around the Sun, it is worth studying the prospects for planet

formation in this environment. Planet formation models are divided into two categories: gravitational instabilities (25) and core accretion (26). It seems improbable that giant planets will form by means of gravitational instabilities, because the Toomre stability criterion coefficient, equal to  $H_g/r M_\odot/(r^2\Sigma)$ , is  $\gg 1$  (27). Considering the alternative core accretion scenario by which planets coagulate from initially  $\mu\text{m}$ -sized dust (28, 29), it also appears improbable that cores of giant planets are present in the outer regions because of the very long local orbital time scales. Although regions within 40 AU have not been resolved by our observations, it is tempting to extrapolate the surface density from the outer regions and investigate the predictions of planet formation models for the inner regions; inside 10 AU, planetary embryos may be present. Follow-up observations at higher angular resolution with the mid-IR instrument of the ESO Very Large Telescope interferometer will allow probing these regions.

#### References and Notes

1. The Extrasolar Planet Encyclopaedia presents a comprehensive list of all known exoplanets ([www.obspm.fr/planets](http://www.obspm.fr/planets)).
2. C. R. O'Dell, S. V. W. Beckwith, *Science* **276**, 1355 (1997).
3. A comprehensive list of spatially resolved disks is available ([www.circumstellardisks.org](http://www.circumstellardisks.org)).
4. J. S. Greaves, *Science* **307**, 68 (2005).
5. T. Takeuchi, C. J. Clarke, D. N. C. Lin, *Astrophys. J.* **627-1**, 286 (2005).
6. J. Setiawan et al., *Astron. Astrophys.* **437**, L31 (2005).
7. B. A. Smith, R. J. Terrell, *Science* **226**, 1421 (1984).
8. G. Meeus et al., *Astron. Astrophys.* **365**, 476 (2001).
9. E. I. Chiang et al., *Astrophys. J.* **547**, 1077 (2001).
10. V. Mannings, A. I. Sargent, *Astrophys. J.* **529**, 391 (2000).
11. C. Grady et al., *Astrophys. J.* **630**, 958 (2005).
12. B. Acke, M. E. van den Ancker, *Astron. Astrophys.* **426**, 151 (2004).
13. J. L. Puget, A. Leger, *Annu. Rev. Astron. Astrophys.* **27**, 161 (1989).
14. P.-O. Lagage et al., *The Messenger* **117**, 12 (2004).
15. M. E. van den Ancker, D. de Winter, H. R. E. Tjin A Djie, *Astron. Astrophys.* **330**, 145 (1998).
16. C. Van Kerkhoven, A. G. G. Tielens, C. Waelkens, *Astron. Astrophys.* **384**, 568 (2002).
17. T. Prusti, A. Natta, F. Palla, *Astron. Astrophys.* **292**, 593 (1994).
18. R. van Boekel et al., *Astron. Astrophys.* **418**, 177 (2004).
19. V. Ossenkopf, Th. Henning, *Astron. Astrophys.* **291**, 943 (1994).
20. S. J. Weidenschilling, *Astrophys. Space Sci.* **51**, 153 (1977).
21. M. J. Kuchner, *Astrophys. J.* **612**, 1147 (2004).
22. Th. Henning, A. Burkert, R. Launhardt, Ch. Leinert, B. Stecklum, *Astron. Astrophys.* **336**, 565 (1998).
23. P. Artymowicz, *Annu. Rev. Earth Planet. Sci.* **25**, 175 (1997).
24. J. S. Weintraub, J. S. Bary, J. H. Kastner, S. J. Shukla, K. Chynoweth, in *Proceedings of the Protostars and Planets V Conference*, Waikoloa, HI, 24 to 28 October, 2005, B. Reipurth, D. Jewitt, K. Keil, Eds. (LPI Contribution Number 1286, Univ. Arizona Press, Tucson, 2006), p. 8197.
25. R. H. Durisen et al., in *Protostars and Planets V*, B. Reipurth, D. Jewitt, K. Keil, Eds. (Univ. of Arizona Press, Tucson, 2006), in press; preprint ([www.ifa.hawaii.edu/UHNAI/ppv.htm](http://www.ifa.hawaii.edu/UHNAI/ppv.htm)).
26. J. J. Lissauer, *Annu. Rev. Astron. Astrophys.* **31**, 129 (1993).
27. A. Toomre, *Astrophys. J.* **139**, 1217 (1964).
28. S. Ida, D. N. C. Lin, *Astrophys. J.* **604-1**, 388 (2004).
29. P. Goldreich, Y. Lithwick, R. Sari, *Astrophys. J.* **614-1**, 497 (2004).
30. This work was based on observations carried out at the ESO, Paranal, Chile. The VISIR could not have been built without contributions from many people, including G. Durand, Y. Rio, M. Authier, C. Lyraud, and J. Pragt. We also thank A. Palacio, P. Nighiem, and C. Martin for discussions about the age of HD 97048, as well as F. Masset for discussions about gravitational instabilities.

#### Supporting Online Material

[www.sciencemag.org/cgi/content/full/1131436/DC1](http://www.sciencemag.org/cgi/content/full/1131436/DC1)  
Figs. S1 and S2

19 June 2006; accepted 12 September 2006  
Published online 28 September 2006;  
10.1126/science.1131436  
Include this information when citing this paper

## The Phase-Dependent Infrared Brightness of the Extrasolar Planet $\upsilon$ Andromedae b

Joseph Harrington,<sup>1,2</sup> Brad M. Hansen,<sup>3\*</sup> Statia H. Luszcz,<sup>2,4</sup> Sara Seager,<sup>5</sup> Drake Deming,<sup>6</sup> Kristen Menou,<sup>7</sup> James Y.-K. Cho,<sup>8</sup> L. Jeremy Richardson<sup>9</sup>

The star  $\upsilon$  Andromedae is orbited by three known planets, the innermost of which has an orbital period of 4.617 days and a mass at least 0.69 that of Jupiter. This planet is close enough to its host star that the radiation it absorbs overwhelms its internal heat losses. Here, we present the 24-micrometer light curve of this system, obtained with the Spitzer Space Telescope. It shows a variation in phase with the orbital motion of the innermost planet, demonstrating that such planets possess distinct hot substellar (day) and cold antistellar (night) faces.

Last year, two independent groups (1, 2) reported the first measurements of the infrared light emitted by extrasolar planets orbiting close to their parent stars. These “hot Jupiter” (3) planets have small enough orbits that

the energy they absorb from their hosts dominates their own internal energy losses. How they absorb and reradiate this energy is fundamental to understanding the behavior of their atmospheres. One way to address this question is to monitor the

emitted flux over the course of an orbit to see whether the heat is distributed asymmetrically about the surface of the planet.

We have observed the  $\upsilon$  Andromedae system with the 24- $\mu\text{m}$  channel of the Multiband Imaging Photometer for Spitzer (MIPS) (4) aboard the Spitzer Space Telescope (5). We took 168 3-s images at each of five epochs spread over 4.46 days (97% of the 4.617-day orbital period of  $\upsilon$  Andromedae b) beginning on 18 February 2006 at 12:52 UTC. After rejecting frames with bad pixels near the star and those with Spitzer’s “first frame effect” (1) (2% to 8% of the data, depending on epoch), we measured the flux of the system and that of the surrounding sky by using both subpixel, interpolated aperture photometry and optimal photometry (6, 7) on each frame.

The detection of eclipses (8) from the hot Jupiter planetary systems HD 209458b (1), TrES-1 (2), and HD 189733b (9) demonstrate that a small fraction ( $\sim 0.1\%$ ) of the total infrared light we observe from these systems is actually emitted from the planet rather than the

## Anatomy of a Flaring Proto-Planetary Disk Around a Young Intermediate-Mass Star

Pierre-Olivier Lagage, Coralie Doucet, Eric Pantin, Emilie Habart, Gaspard Duchêne, François Ménard, Christophe Pinte, Sébastien Charnoz and Jan-Willem Pel

*Science* **314** (5799), 621-623.

DOI: 10.1126/science.1131436originally published online September 28, 2006

### ARTICLE TOOLS

<http://science.sciencemag.org/content/314/5799/621>

### SUPPLEMENTARY MATERIALS

<http://science.sciencemag.org/content/suppl/2006/09/26/1131436.DC1>

### RELATED CONTENT

<http://science.sciencemag.org/content/sci/314/5799/605.full>

### REFERENCES

This article cites 25 articles, 3 of which you can access for free  
<http://science.sciencemag.org/content/314/5799/621#BIBL>

### PERMISSIONS

<http://www.sciencemag.org/help/reprints-and-permissions>

Use of this article is subject to the [Terms of Service](#)